Available online at www.sciencedirect.com
ScienceDirect
Ceramics International 38 (2012) 503–509
CERAMICS INTERNATIONAL
www.elsevier.com/locate/ceramint

A comparative study on UV light activated porous TiO_2 and ZnO film sensors for gas sensing at room temperature

Hao Chen, Yuan Liu, Changsheng Xie *, Jun Wu, Dawen Zeng, Yichuan Liao

State Key Laboratory of Material Processing and Die & Mould Technology, Nanomaterials and Smart Sensors Laboratory, Department of Materials Science and Engineering, Huazhong University of Science and Technology, Wuhan 430074, PR China

Received 23 May 2011; received in revised form 18 July 2011; accepted 19 July 2011
Available online 26th July 2011

Abstract

In order to find a new approach for screening the photoactivated gas sensing materials with high sensitivity, a comparative study was carried out. With the simple technique of screen printing, TiO_2 and ZnO were used to fabricate the UV light activated gas sensors which were applied at room temperature. To facilitate the simultaneous measurements of the current transients of the two materials, they were printed on the same alumina substrate. Compared with ZnO, TiO_2 exhibited a superior performance to ethanol and formaldehyde gases. It was found that the responses of TiO_2 increased with the concentration of test gas and amounted to 224 and 1700 to 100 ppm ethanol and formaldehyde gases, respectively, while the responses of ZnO to 100 ppm ethanol and formaldehyde gases were 0.14 and 1.5, respectively. The mechanism of such a huge difference between TiO_2 and ZnO was discussed in detail. Furthermore, it is suggested that metal oxide semiconductor with lower photo-to-dark current ratio can achieve higher photoactivated gas sensitivity.

Keywords: D. TiO_2; D. ZnO; Photoactivated; Gas sensor; Sensitivity; Comparative study

1. Introduction

Chemical sensor is an effective way to detect pollutant, toxic and combustible gases. Therefore, a lot of effort has been focused on this field [1–3]. The conventional metal oxide gas sensors are activated by heat, generally working at a temperature between 200 and 400 °C, which limits their applications to flammable gases and some special conditions such as being as biosensors [2]. Compared with heat-activated metal oxide gas sensors, photoactivated gas sensors do not need to be heated so that they can work at room temperature, which expands their applications and also avoids the long-term instability caused by diffusion and sintering effects on metal oxide grain boundaries [4,5].

So far, there are a few reports of photoactivated metal oxide gas sensors. Comini et al. have reported the effects of UV light illumination on the performances of SnO_2 and In_2O_3 semiconductor gas sensors toward CO and NO_2 [6]. After that, some attentions have been paid to the light enhanced gas sensing phenomenon, and most of them were focused on In_2O_3, SnO_2 [7–9]. Apart from this, there are also a lot of studies on ZnO [4,5,10–12]. Ge et al. discovered the enhancement of the gas-sensing performances of La-doped ZnO nanoparticle to alcohol and benzene with UV-light excitation [10]. Jian et al. reported UV-light activated ZnO fibers for organic gas sensing at room temperature [4], in which the abnormal response was discovered. Among these studies, many preparation methods have been attempted and sensors with various morphology have been fabricated, such as morphology with high specific surface area (fibers [4], nanowire [5]), doping with other elements [10], etc. However, most of them did not get gas sensor with high sensitivity and the manufacturing processes were complex.

In this study, we have chosen two kinds of metal oxides for comparative study. One is TiO_2 and the other is ZnO. Since TiO_2 is a well known photocatalyst. According to the consistency of photocatalytic reaction and photoactivated gas sensing process, we deduced that TiO_2 might be an excellent photoactivated gas sensor. And the gas sensitivity of ZnO was widely investigated, so we selected ZnO as a comparison in order to investigate the relationship between sensitivities and materials so as to conduct the screening of photoactivated gas sensing materials with high sensitivity.

* Corresponding author. Tel.: +86 27 8755 6544; fax: +86 27 8754 3778.
E-mail address: csxie@mail.hust.edu.cn (C. Xie).

0272-8842/$36.00
doi:10.1016/j.ceramint.2011.07.035

2. Experimental

2.1. Samples preparation

TiO_2 (Degussa P25, average grain size: 30 nm) and ZnO (Shenzhen Zunye Nanomaterials Co. Ltd. average grain size: 80 nm) were used in this study. To gain the pastes which were suitable for screen printing to make the sensors, we have used ball milling technique to homogeneously mix the above two kinds of material with a certain amount of organic solvent (composed of terpineol, butyl carbitol, ethyl-cellulose, span 85 and din-butyl phthalate), respectively. Afterwards, the pastes were printed by screen printing onto the Au interdigital electrodes which were preprinted on the same alumina substrate, and the thickness of each film which was controlled by the screen printing machine was 10 μm [13,14]. The screen printing method can ensure the consistency of the sensors so they can be easily reproduced.

Then, the samples were dried for 30 min at 80 °C in an oven. After drying, in order to eliminate the organic solvent, these samples were heat treated successively for 30 min at 250 °C. In the end, the printed samples were transferred into the furnace and sintered at 550 °C for 2 h in air. All the preparation procedures were the same as our previous work [13], the purpose of these procedures were to improve the mechanical bond of particles of the sensors so that the films could not fall off easily. A flat-plate type device printed with two sensors was obtained as shown in Fig. 1.

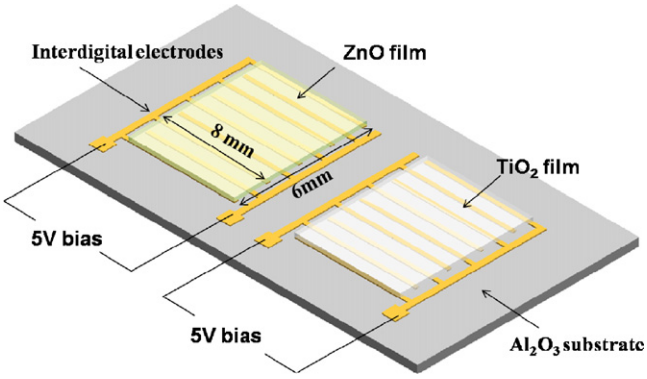

Fig. 1. The flat-plate type device printed with ZnO and TiO_2.

2.2. The testing process of gas sensing response

Fig. 2 shows the schematic diagram of the platform for the test of gas sensing response. The platform was consisted of gas channels and electric circuits.

Gas channels. Dry air was supplied by air generator (Beijing Keep-Science Analysis SCI&TECH Co.) and each kind of test gas was prepared by mixing the test liquid into compressed air. The gas fluxes of test gas and dry air were controlled by computer through the mass flow controllers.

Electric circuits. Data acquisition card (PCI-6225, National Instrument Co.) provided 5 V biases on the sensors and measured the current transients of them. LED array light source (Shenzhen Ti-Times Co.) which was controlled by computer provided the ultraviolet (365 nm, 36 W/m^2).

Before each test, the sensors must be heated and blown with a dryer for 10 min, with the heating temperature of ca. 38 °C, which could not only eliminate effects of the humidity or reactions on the testing process but also minimized the effects of heat on recovery process. Afterwards, we kept the mass flow controller which controlled dry air opened for 10 min to flush out the test chamber. Then the testing processes began and computer started recording data. Take Fig. 3 (current transients of TiO_2 and ZnO under 75 ppm formaldehyde gas) as an example to illustrate the testing process. Initially, the dry air was opened and kept flowing throughout the subsequent testing process; 5 V bias voltages were loaded at 15 s; at 30 s, the light source was on; at 180 s, mass flow controller which controlled test gas was opened so as to introduce the test gas into the test chamber; at 330 s, test gas was closed; at 500 s, the light source was off; at 600 s, the bias voltages were unloaded and the test was finished. The response value of the sensors were defined as $S = (I_g - I_p)/I_p$ (where I_p and I_g were the photocurrents amplitude before and after the introduction of test gas, which were obtained at 180 s and 330 s, respectively.). During the tests of TiO_2, it was found that I_p were

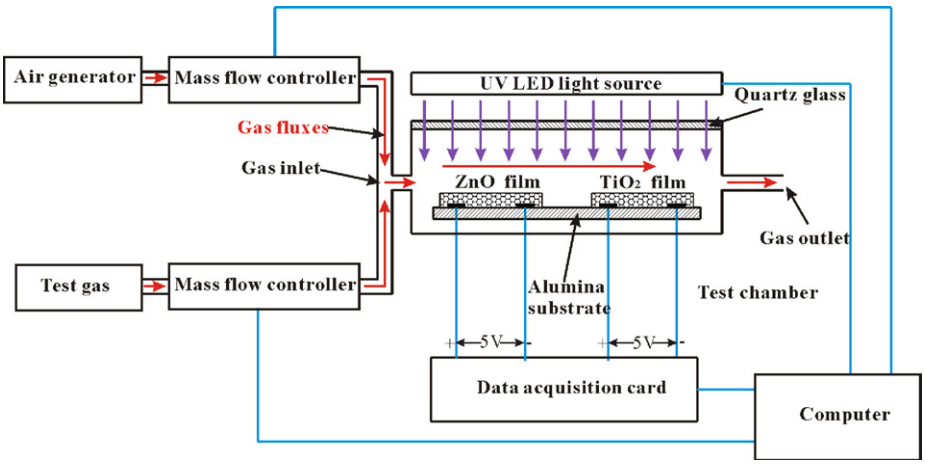

Fig. 2. Schematic diagram of the platform for gas sensing response testing. Red arrows denote gas fluxes, violet arrows denote UV light, and blue lines denote electric wires. (For interpretation of the references to color in this figure legend, the reader is referred to the web version of this article.)

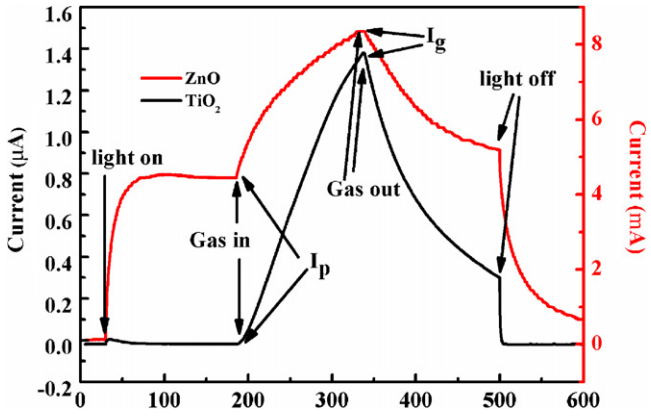

Fig. 3. The testing process (current transients of TiO_2 and ZnO under 75 ppm formaldehyde gas) and the definition of I_p and I_g.

nearly a constant, whereas I_g increased more and more as the tests were repeated and finally reached saturation. Hence, to avoid the effect of the number of tests on I_g, we only take the maximum of I_g in the determination of S.

3. Results and discussion

3.1. Structure characterization

Fig. 4(a) and (b) show the scanning electron micrograph (SEM) images of TiO_2 and ZnO, respectively. As seen that the

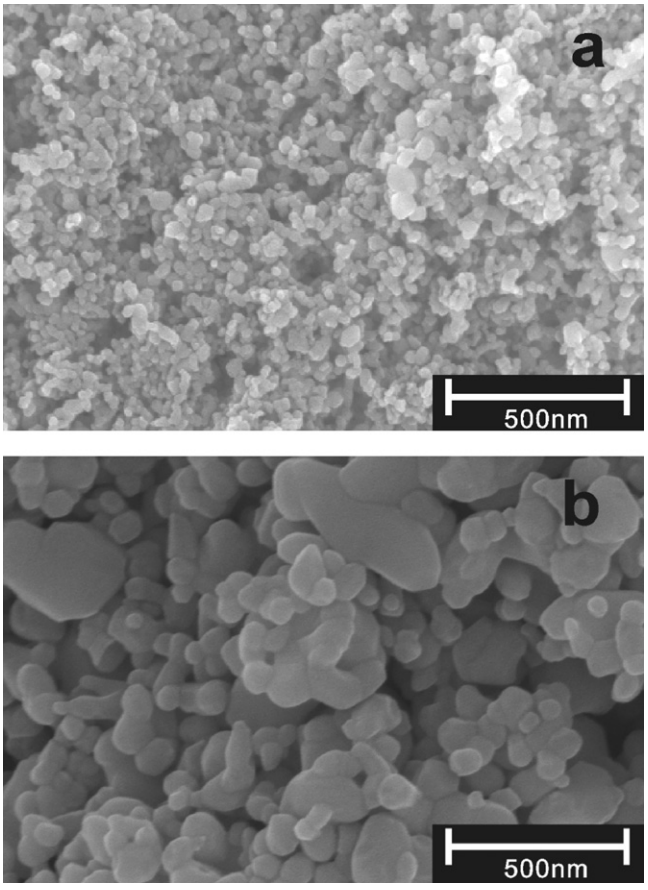

Fig. 4. The scanning electron micrograph (SEM) images of (a) TiO_2 and (b) ZnO.

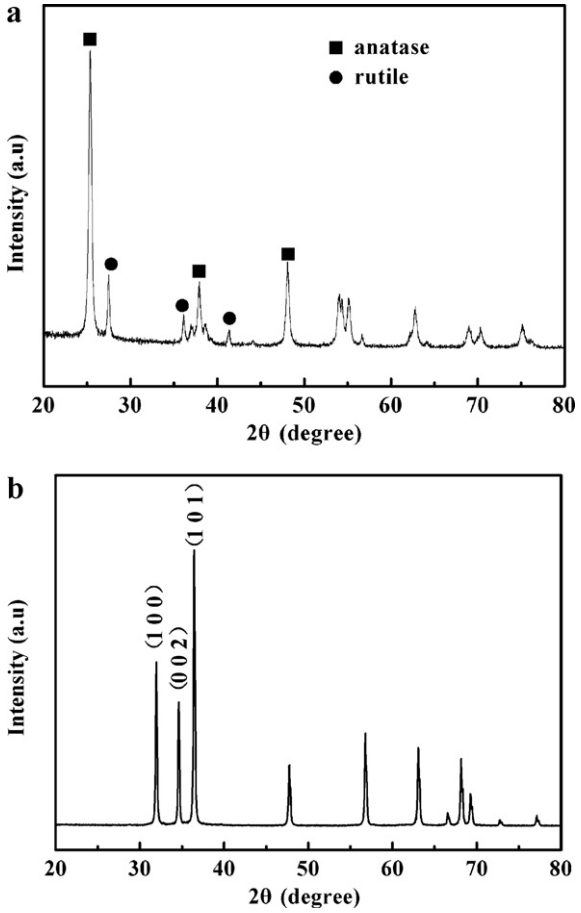

Fig. 5. X-ray diffraction (XRD) patterns of (a) TiO_2 and (b) ZnO.

average grain sizes of TiO_2 and ZnO were ca. 30 nm and 80 nm, respectively, which were consistent with raw materials. Therefore, the ball milling and screen printing techniques barely changed the morphology of raw materials. The films fabricated by screen printing were porous structures which were suitable for reacting with test gases. Fig. 5(a) and (b) exhibit the X-ray diffraction (XRD) patterns of TiO_2 and ZnO, respectively, indicating that, in common with the phases of raw materials, TiO_2 was consisted of anatase and rutile while ZnO was consisted of wurtzite.

3.2. UV light activated gas sensing process

Fig. 6 shows under UV light irradiation, current transients (Fig. 6(a)) of TiO_2 under different concentrations of ethanol gas as well as the corresponding response values (Fig. 6(b)). Meanwhile Fig. 7 shows those of TiO_2 under different concentrations of formaldehyde gas. All the current transients consist of four characteristic regions: (i) a low current region before UV light irradiation, (ii) under UV light irradiation, a fast but small increment and then falls to a steady state value that is around 10 times the dark current, (iii) a quasi-linear increase under test gas exposure, (iv) a quasi-linear decrease after turning off the test gas. Region (iii) and (iv) suggest good response and recovery capacity of TiO_2 sensor. It is observed that the responses increased with the concentration of test gases

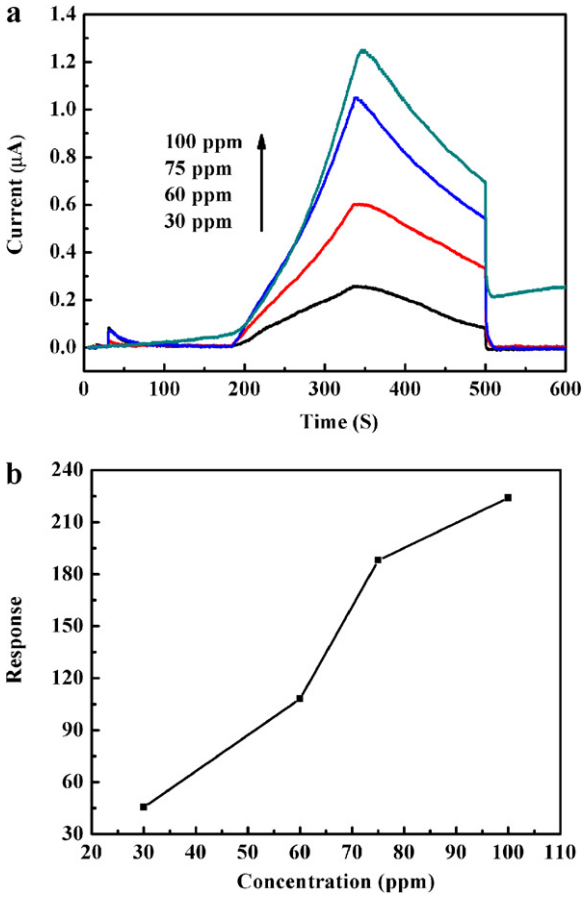

Fig. 6. (a) Current transients of TiO_2 under different concentrations of ethanol gas and UV light irradiation, (b) the variation of the response values with the concentration of ethanol gas.

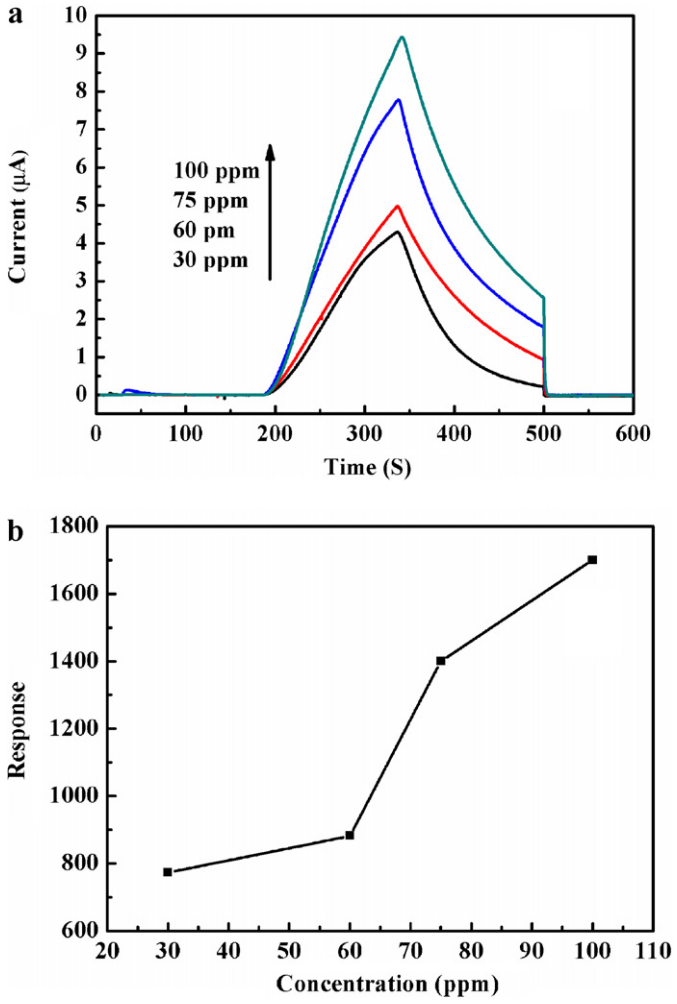

Fig. 7. (a) Current transients of TiO_2 under different concentrations of formaldehyde gas and UV light irradiation, (b) the variation of the responses values with the concentration of formaldehyde gas.

increasing and have achieved 224 and 1700 to 100 ppm ethanol and formaldehyde gases, respectively. The response to formaldehyde gas is much larger than that of ethanol gas of the same concentration, which might be owing to that the photocatalytic reaction of formaldehyde is rapid than that of ethanol.

In marked contrast to the behavior of TiO_2, the simultaneous measured current transients of ZnO were very different. Under UV light irradiation, the currents of ZnO increased about 200–1000 times than in the dark. However, the photocurrents increased slightly with the concentrations of test gases. The responses of ZnO to low concentrations (30–75 ppm) of ethanol gas were so low that they could not be detected clearly. Consequently, Fig. 8 only shows the current transient of ZnO under 100 ppm ethanol gas. As shown in Fig. 9(a), in the tests of ZnO to formaldehyde gas, I_p were different, so in the determination of response values they were replaced by $\bar{I}_p$ which was calculated by averaging I_p of four different concentrations. The maximum response was 1.5 as shown in Fig. 9(b). The results are consistent with other studies of ZnO, in which the response values at similar conditions were from ca. 0.1 [5] to no more than 4 [10], indicating that the photoactivated sensitivities of ZnO are low. Furthermore, the references cited in the introduction have reported various photo-activated gas sensors with different particle sizes and morphologies of ZnO

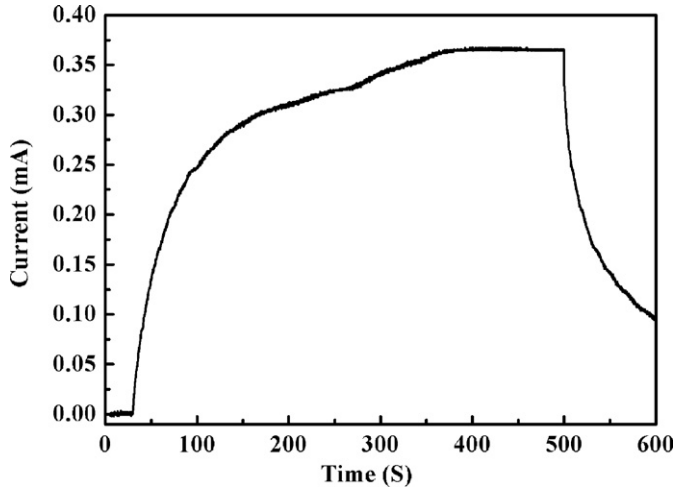

Fig. 8. Current transient of ZnO under 100 ppm ethanol gas.

particles. However, the sensitivities of ZnO are all much lower than those of TiO_2 in this study. In our opinion, the slight difference in particle size (ZnO ca.80 nm, TiO_2 ca. 30 nm) should not be responsible for major differences in gas sensing,

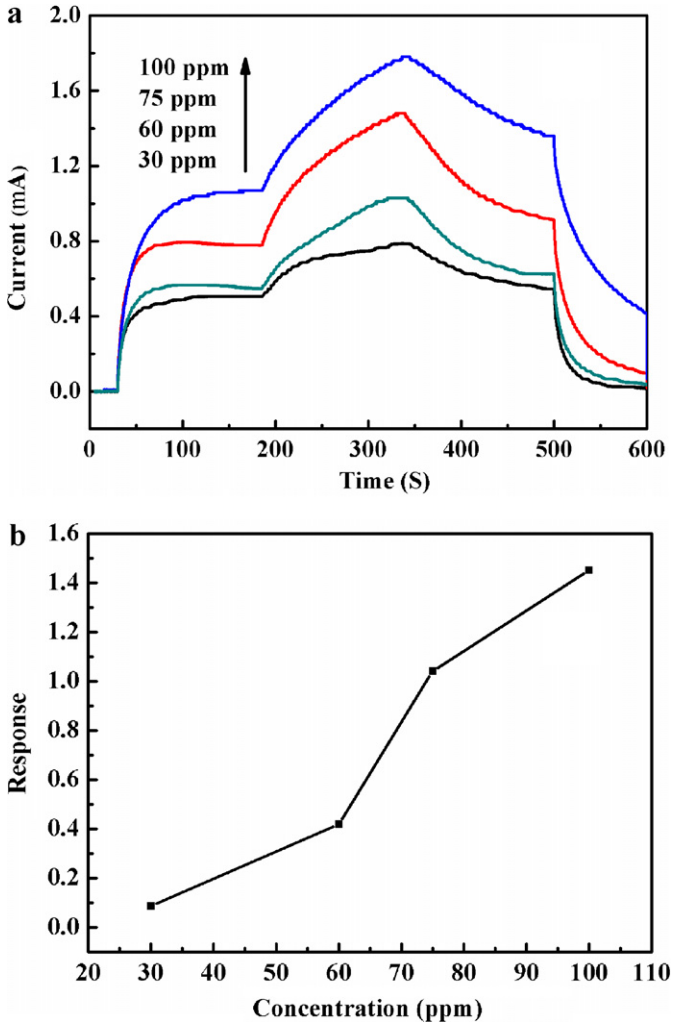

Fig. 9. (a) Current transients of ZnO under different concentrations of formaldehyde gas and UV light irradiation; (b) the variation of response values with the concentration of formaldehyde gas.

and possibly also in photo to dark responses of porous ZnO and TiO_2 films.

3.3. Explanations on the differences between TiO_2 and ZnO sensors

According to the test process, we divided the differences between ZnO and TiO_2 sensors into two parts: photo response process and photocatalytic reaction process which happened before and after the introduction of test gas, respectively.

3.3.1. Photo response process

Photo response process is a preparation of the photocatalytic reaction process, so it is helpful to elucidate this matter before discussing the photocatalytic reaction process. Fig. 10 shows the schematic of double Schottky barrier models of porous sensing films under different conditions. As shown in Fig. 10(a), before UV light irradiation, due to the reaction

$$e^- + O_2(g) \rightarrow O_2^-(ad) \quad (1)$$

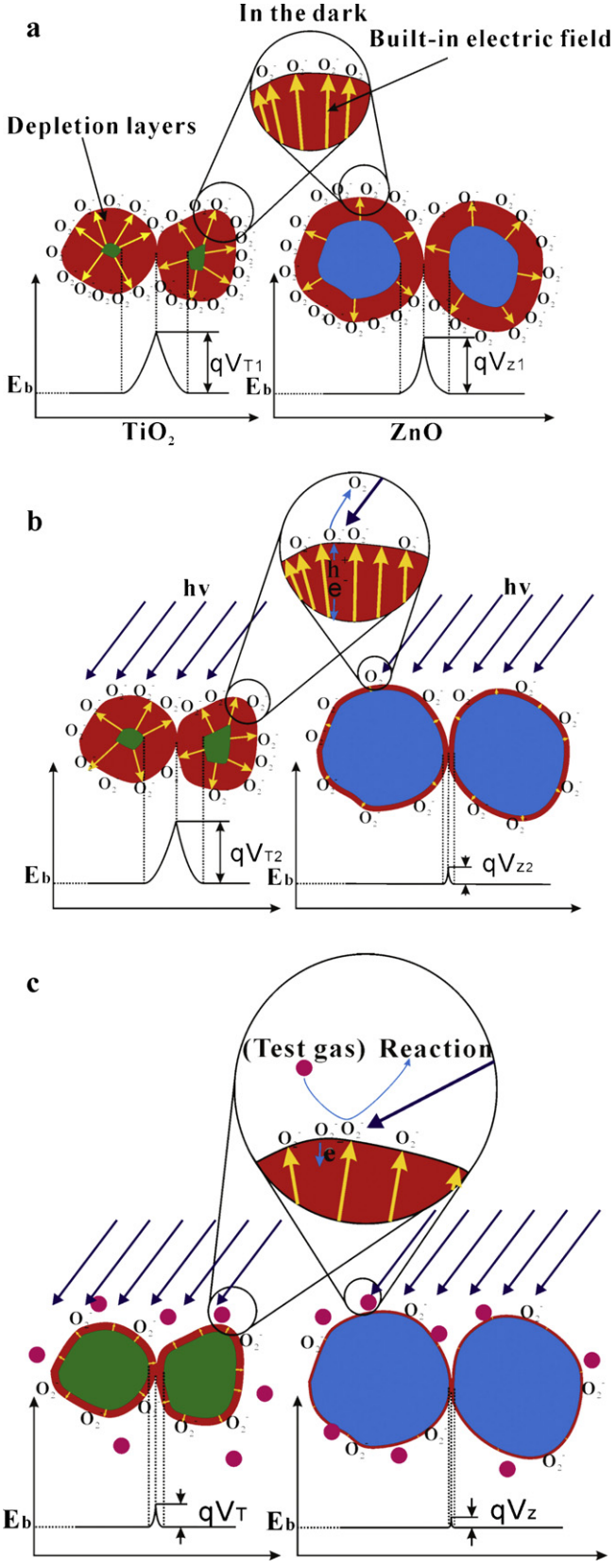

Fig. 10. Schematic of surface reactions and the corresponding energy barriers (qV_T and qV_Z, in which q is electron charge and V_T, V_Z are potential barriers of TiO_2 and ZnO, respectively) under different conditions: (a) in dry air and in the dark, (b) in dry air and with UV light illumination, (c) in test gas and with UV light illumination.

large amount of O_2^- absorbed on the surface of the sensors [15], which induced the formation of depletion layers, built-in electric fields [16,17] and energy barriers (qV_T and qV_Z, in which q is electron charge and V_T, V_Z are potential barriers of TiO_2 and ZnO, respectively). Hence, sensors exhibited low dark currents. Upon UV irradiation, photogenerated holes and electrons appeared, and then they were separated under the effect of the built-in electric fields, which is shown in Fig. 10(b). Due to the built-in electric fields, electrons migrated inside of the particles while the holes remained on the surfaces or migrated to the surfaces and reacted with O_2^- [17], which induced the desorption of O_2^-, described by reaction

$$h^+ + O_2^-(\text{ad}) \rightarrow O_2(\text{g}) \quad (2)$$

resulting in diminishments of depletion layers and increments in currents. Eventually, the currents reached saturations due to the competition between reaction (1) and reaction (2).

In this study, under UV light irradiation, the current increments of TiO_2 are much smaller than that of ZnO, indicating that there are large amount of O_2^- on the surface of TiO_2 sensor while there are only small amount of O_2^- on the surface of ZnO sensor. The results are consistent with other studies where although there are some differences in morphology and light intensity, which can be ignored in view of their dramatic difference in photo-to-dark current ratios, the photo-to-dark current ratio of TiO_2 is ca. 10 [18,19] while that of ZnO is ca. 10^5 [20]. Because of the similar band structures of TiO_2 and ZnO [21] and their large difference in carrier mobility [18,22], we ascribe the difference to the latter which influence the rate of electrons move to the inside of the particles and holes move to the surface of the particles, which might affect the rate of reaction (1) and (2). However, further study is still needed.

3.3.2. Photocatalytic reaction process

In Fig. 10(c), with UV light irradiation, test gas was introduced into the test chamber and reacted with O_2^- as follows [23]:

$$CH_3CH_2OH + O_2^-(\text{ad}) \rightarrow CO_2 + H_2O + e^- \quad (3)$$

$$CH_2O + O_2^-(\text{ad}) \rightarrow CO_2 + H_2O + e^- \quad (4)$$

These reactions released electrons, which could enhance the carrier densities. Moreover, before the introduction of test gas, there had been a large amount of O_2^- reserved on TiO_2 particles, so when the test gas was introduced, O_2^- were removed greatly, which induced a great thinning of depletion layer and a high increase of current. Therefore, TiO_2 exhibited large response to test gas. In contrast, there were small amounts of O_2^- on the surface of ZnO particles before the introduction of test gas, so the depletion layer on ZnO was thin and the removal of O_2^- on ZnO particles by photocatalytic reaction have only a small effect on the thickness of depletion layer, which induced a small response value.The response values in this study are in good agreement with the enlargements of photocurrents under vacuum reported by other investigations, in which the photocurrents of ZnO under vacuum were about several times [24,25] of magnitude larger than in air, indicating that there were only a small amount of O_2^- absorbed on the surface of ZnO sensor to be removed under vacuum. In contrast, the photocurrents of TiO_2 under vacuum were about 10^3 [19] to 10^6 [26] times larger than in air, indicating that there were many residual O_2^- on TiO_2 particles when TiO_2 were exposed in air and with UV light illumination. Therefore, the removals of O_2^- by irradiation under vacuum have the same effects as photocatalytic reactions. The more O_2^- is absorbed by the surface of the sensor, the higher sensitivity it is. From this point of view, as well as taking the relationship between photo-to-dark current ratio and the amount of absorbed O_2^- into account, we concluded that the sensor with lower photo-to-dark current ratio is more likely to get higher photoactivated gas sensitivity.

4. Conclusion

In this study, with the purpose of directing the choice of photoactivated gas sensing materials, we have fabricated two kinds of UV light activated gas sensors working at room temperature with TiO_2 and ZnO, using the simple technique of screen printing. The response values of TiO_2 to ethanol and formaldehyde gases were much larger than those of ZnO and the response values of TiO_2 to 100 ppm ethanol and formaldehyde gases have achieved 224 and 1700, respectively. Consequently, TiO_2 might be a hopeful material for the photo-activated gas sensor.

The different gas sensing responses between TiO_2 and ZnO were caused by the different quantity of O_2^- absorbed on the surfaces of the sensors under UV light irradiation, which was educed from their huge difference in photo-to-dark current ratios. There were large amounts of residual O_2^- reserved on the surface of TiO_2 sensor under UV light irradiation, so the significant reduction of them by photocatalytic reaction results in a tremendous growth in photocurrent. However, there were few O_2^- reserved on the surface of ZnO sensor, so the diminishment of them cannot have an huge impact on the photocurrent. Through comparing TiO_2 and ZnO, and referring to other investigations, a novel conception that the material with low photo-to-dark current ratio is more likely to get high photoactivated gas sensitivity, is proposed.

Acknowledgements

This work was supported by the Nature Science Foundation of China (No. 50927201) and the National Basic Research Program of China (Grant Nos. 2009CB939705 and 2009CB939702). The authors are also grateful to Analytical and Testing Center of Huazhong University of Science and Technology.

References

[1] J. Kong, N. Franklin, C. Zhou, M. Chapline, S. Peng, K. Cho, H. Dai, Nanotube molecular wires as chemical sensors, Science 287 (2000) 622.
[2] C. Grimes, Synthesis and application of highly ordered arrays of TiO_2 nanotubes, Journal of Materials Chemistry 17 (2007) 1451–1457.
[3] B. Zhu, C. Xie, W. Wang, K. Huang, J. Hu, Improvement in gas sensitivity of ZnO thick film to volatile organic compounds (VOCs) by adding TiO_2, Materials Letters 58 (2004) 624–629.

[4] J. Gong, Y.H. Li, X.S. Chai, Z.S. Hu, Y.L. Deng, UV-light-activated ZnO fibers for organic gas sensing at room temperature, Journal of Physical Chemistry C 114 (2010) 1293–1298.
[5] S.W. Fan, A.K. Srivastava, V.P. Dravid, UV-activated room-temperature gas sensing mechanism of polycrystalline ZnO, Applied Physics Letters 95 (2009) 142106.
[6] E. Comini, A. Cristalli, G. Faglia, G. Sberveglieri, Light enhanced gas sensing properties of indium oxide and tin dioxide sensors, Sensors and Actuators B: Chemical 65 (2000) 260–263.
[7] K. Anothainart, M. Burgmair, A. Karthigeyan, M. Zimmer, I. Eisele, Light enhanced NO_2 gas sensing with tin oxide at room temperature: conductance and work function measurements, Sensors and Actuators B: Chemical 93 (2003) 580–584.
[8] E. Comini, G. Faglia, G. Sberveglieri, UV light activation of tin oxide thin films for NO_2 sensing at low temperatures, Sensors and Actuators B: Chemical 78 (2001) 73–77.
[9] J.D. Prades, R. Jimenez-Diaz, F. Hernandez-Ramirez, S. Barth, A. Cirera, A. Romano-Rodriguez, S. Mathur, J. Morante, Equivalence between thermal and room temperature UV light-modulated responses of gas sensors based on individual SnO_2 nanowires, Sensors and Actuators B: Chemical 140 (2009) 337–341.
[10] C. Ge, C. Xie, M. Hu, Y. Gui, Z. Bai, D. Zeng, Structural characteristics and UV-light enhanced gas sensitivity of La-doped ZnO nanoparticles, Materials Science and Engineering: B 141 (2007) 43–48.
[11] B. de Lacy Costello, R. Ewen, N.M. Ratcliffe, M. Richards, Highly sensitive room temperature sensors based on the UV-LED activation of zinc oxide nanoparticles, Sensors and Actuators B: Chemical 134 (2008) 945–952.
[12] J. Zhai, D. Wang, L. Peng, Y. Lin, X. Li, T. Xie, Visible-light-induced photoelectric gas sensing to formaldehyde based on CdS nanoparticles/ZnO heterostructures, Sensors and Actuators B: Chemical 147 (2010) 234–240.
[13] Z.J. Zou, Y. Liu, H.Y. Li, Y.C. Liao, C.S. Xie, Synthesis of $TiO_2/WO_3/MnO_2$ composites and high-throughput screening for their photoelectrical properties, Journal of Combinatorial Chemistry 12 (2010) 363–369.
[14] Y. Liu, C. Xie, H. Li, H. Chen, Y. Liao, D. Zeng, Low bias photoelectrocatalytic (PEC) performance for organic vapour degradation using TiO_2/WO_3 nanocomposite, Applied Catalysis B: Environmental 102 (2011) 157–162.
[15] Y. Muraoka, N. Takubo, Z. Hiroi, Photoinduced conductivity in tin dioxide thin films, Journal of Applied Physics 105 (2009) 103702.
[16] C.H. Lin, R.S. Chen, T.T. Chen, H.Y. Chen, Y.F. Chen, K.H. Chen, L.C. Chen, High photocurrent gain in SnO_2 nanowires, Applied Physics Letters 93 (2008) 112115.
[17] J.D. Prades, F. Hernandez-Ramirez, R. Jimenez-Diaz, M. Manzanares, T. Andreu, A. Cirera, A. Romano-Rodriguez, J.R. Morante, The effects of electron–hole separation on the photoconductivity of individual metal oxide nanowires, Nanotechnology 19 (2008) 465501.
[18] H. Tang, K. Prasad, R. Sanjines, P. Schmid, F. Levy, Electrical and optical properties of TiO_2 anatase thin films, Journal of Applied Physics 75 (1994) 2042–2047.
[19] A. Brajsa, K. Szaniawska, R.J. Barczynski, L. Murawski, B. Koscielska, A. Vomvas, K. Pomoni, The photoconductivity of sol-gel derived TiO_2 films, Optical Materials 26 (2004) 151–153.
[20] D. Zhang, D. Brodie, Effects of annealing ZnO films prepared by ion-beam-assisted reactive deposition, Thin Solid Films 238 (1994) 95–100.
[21] Y. Xu, M. Schoonen, The absolute energy positions of conduction and valence bands of selected semiconducting minerals, American Mineralogist 85 (2000) 543.
[22] D.R. Lide, CRC Handbook of Chemistry and Physics, CRC Pr I Llc, Boca Roton, FL, 2003.
[23] D.S. Muggli, J.T. McCue, J.L. Falconer, Mechanism of the photocatalytic oxidation of ethanol on TiO_2, Journal of Catalysis 173 (1998) 470–483.
[24] J. Nayak, J. Kasuya, A. Watanabe, S. Nozaki, Persistent photoconductivity in ZnO nanorods deposited on electro-deposited seed layers of ZnO, Journal of Physics: Condensed Matter 20 (2008).
[25] S. Studenikin, N. Golego, M. Cocivera, Carrier mobility and density contributions to photoconductivity transients in polycrystalline ZnO films, Journal of Applied Physics 87 (2000) 2413.
[26] A.A. Eppler, I.N. Ballard, J. Nelson, Charge transport in porous nanocrystalline titanium dioxide, Physica E 14 (2002) 197–202.